

# Unraveling the pion light-cone distribution function in the CEPC era

Yao Ji<sup>1,\*</sup> and Yu-Ming Wang<sup>2,\*\*</sup>

<sup>1</sup>Physik Department T31, James-Frank-Straße 1, Technische Universität München, D-85748 Garching, Germany

<sup>2</sup>School of Physics, Nankai University, Weijin Road 94, 300071 Tianjin, China

## Abstract.

The light-cone distribution amplitude (LCDA) encapsulates the nonperturbative information of the hadronic states in hard exclusive reactions. The envisioned Circular Electron Positron Collider (CEPC) has the potential to access the pion LCDA at an unprecedented level of accuracy with its clean background, broad energy range, high luminosity and precision measurements. Such knowledge can not only deepen our understanding of the composite hadron structure, but also provide new insights for exploring the intricate structures of the underlying non-abelian gauge theory (QCD).

## 1 Introduction

It is well known that the parton distribution function (PDF) provides the nonperturbative ingredient in the study of inclusive hard interactions. Likewise, the light-cone distribution amplitude (LCDA), which admits an amplitude interpretation as the name suggests, is established as the nonperturbative object indispensable for the theoretical studies of hard exclusive processes. While the former has been studied intensively due to its wide application in collider physics and accessibility, the latter has received relatively less attention apart from the recent developments mainly due to the numerical lattice simulation technique (see e.g. [1]). Experimentally, the most promising channels for probing the LCDA of various hadrons are the exclusive photon productions where the envisioned Circular Electron Position Collider (CEPC) certainly provides ample opportunities (see [2] and references therein for technical details). In this report, we aim at addressing the potentiality of the CEPC in the improved determination of the neutral pion LCDA. Together with the pion PDF, they encode rich information on the dynamical structure of the pseudoscalar meson  $\pi^0$  (see [3] for further discussions on probing the flavour-singlet hadrons  $\eta^{(\prime)}$ ).

The exclusive two-photon production of  $\pi^0$  is described via the so-called pion-photon transition form factor (TFF) which has been investigated intensively even before the advent of QCD (see, for instance [4–6]). The interest was fueled at the time mostly because of its role in unveiling the axial anomaly when both incoming photons approach the on-shell limit. The knowledge obtained from the pion TFF in this limit then advanced our understanding of strong interaction and contributed to the development of QCD at its early stage. On the

\*e-mail: yao.ji@tum.de, Preprint Number: TUM-HEP-1433/22.

\*\*e-mail: wangyumnr@nankai.edu.cn

other hand, when one of the photons retains large virtuality, commonly denoted as  $Q^2$ , the pion TFF is predicted to obey the scaling behaviour on the basis of the perturbative factorization theorem. This implies that as  $Q^2$  becomes sufficient large, the TFF is dominated by the leading power contribution generated by the Born amplitude of the collinear light-quark pair production  $\gamma\gamma^* \rightarrow \bar{q}q$ , and the TFF consequently scales as  $1/Q^2$ . It is therefore not surprising that, when the BaBar measurement announced the scaling violation of the pion TFF up to  $Q^2 \sim 40 \text{ GeV}^2$  a decade ago [7], a wave of theoretical investigations were triggered with diverse speculations from both perturbative and nonperturbative sides in an attempt to reconcile the tension between theory and experiment. The experimental data of  $\gamma\gamma^* \rightarrow \pi^0$  are obtained from the ‘‘single-tagged’’ measurements of the differential  $e^+e^- \rightarrow e^+e^-\pi^0$  cross section [7–9], which proves to be more accessible with the BaBar setup.

In order to shed lights on the unexpected scaling violation indicated by the BaBar collaboration and to gain a better control on the perturbative dynamics for extracting the pion LCDA, it is pivotal to pursue the theoretical predictions of the pion TFF to higher orders in the strong coupling  $\alpha_s$ . The foundation for the prediction of the pion TFF at  $Q^2 \gg \Lambda_{\text{QCD}}^2$ , as well as many other two-photon processes such as deeply virtual Compton scattering (DVCS) (see for instance [10–12]) and deeply inelastic lepton-hadron scattering (DIS), consists in operator-product-expansion (OPE) of two time-ordered electromagnetic currents. In the case of  $\gamma\gamma^* \rightarrow \pi^0$ , the OPE technique allows for constructing the factorization formula of the TFF, which is determined by the perturbatively calculable coefficient function (CF) and pion LCDA. Hence with the upcoming improved experimental input for the TFF and the yet more accurate CF, the nonperturbative pion LCDA can be constrained with higher accuracy. Moreover, a better understanding of the pion LCDA also has far-reaching consequences on refining the model-independent description of semileptonic and nonleptonic  $B$ -meson decays such as  $B \rightarrow \pi \ell^- \bar{\nu}_\ell$ ,  $B \rightarrow \pi \ell^+ \ell^-$ ,  $B \rightarrow \pi\pi$  etc (see, e.g., [13–15]). These exclusive heavy-hadron decays in turn hold the key for unraveling the delicate quark-flavour mixing mechanism and for uncovering the ultimate mystery of CP violation.

The CF in the large  $Q^2$  limit had been determined to the next-to-leading order (NLO) in  $\alpha_s$  from the diagrammatic factorization approach more than three decades ago [16–18] (see [19–21] for an alternative treatment by including the non-zero transverse momenta of the active partons). The complete two-loop CF in the  $\overline{\text{MS}}$ -scheme has become available only until very recently with two completely different approaches [22, 23], which however bring about exactly identical results. In what follows, we mainly discuss the prospects of CEPC in the precision determination of the pion LCDA with the most advanced perturbative QCD calculations to date.

## 2 Theory background

The photon-pion transition form factor (TFF)  $F_{\gamma\pi}(Q^2)$  is induced by the electromagnetic current  $j_\mu^{\text{em}}$  sandwiched between an on-shell photon with momentum  $p'$  and the  $\pi^0$  state of momentum  $p$

$$\langle \pi^0(p) | j_\mu^{\text{em}} | \gamma(p') \rangle = g_{\text{em}}^2 \epsilon_{\mu\nu\alpha\beta} q^\alpha p^\beta \epsilon^\nu(p') F_{\gamma\pi}(Q^2), \quad (1)$$

where  $q = p - p'$  refers to the transfer momentum from which the virtuality is defined  $Q^2 = -q^2$ . The totally antisymmetric tensor  $\epsilon_{\mu\nu\alpha\beta}$  with convention  $\epsilon_{0123} = -1$  signifies that  $\pi^0$  is a pseudoscalar meson.  $\epsilon^\nu(p')$  is the polarization vector of the real photon, and  $e_q$  denotes the electric charge of the quark field in units of  $g_{\text{em}} = \sqrt{4\pi\alpha_{\text{em}}}$ . The electromagnetic current is constructed via local quark fields

$$j_\mu^{\text{em}} = \sum_q g_{\text{em}} e_q \bar{q} \gamma_\mu q. \quad (2)$$

It is convenient to introduce two light-cone vectors  $n_\mu$  and  $\bar{n}_\mu$  satisfying  $n^2 = \bar{n}^2 = 0$  and  $n \cdot \bar{n} = 2$ , which permit the decomposition  $p_\mu = (\bar{n} \cdot p)/2 n_\mu$  and  $p'_\mu = (n \cdot p)/2 \bar{n}_\mu$ .

The hard-collinear factorization theorem dictates that the  $\gamma \gamma^* \rightarrow \pi^0$  form factor in the leading-power (LP) approximation <sup>1</sup> can be written as

$$F_{\gamma\pi}^{\text{LP}}(Q^2) = \frac{(e_u^2 - e_d^2)f_\pi}{\sqrt{2} Q^2} \int_0^1 dx T_2(x, Q^2, \mu_F) \phi_\pi(x, \mu_F), \quad (3)$$

where  $f_\pi = (130.2 \pm 1.2)$  MeV is the neutral pion decay constant [24] and  $\mu_F$  represents the factorization scale for which we tacitly take to be the same as the renormalization scale  $\mu_{\text{UV}}$ , i.e.,

$$\mu_F = \mu_{\text{UV}} \equiv \mu. \quad (4)$$

$\phi_\pi(x, \mu_F)$  represents the celebrated (leading-twist) pion LCDA whose scale dependence is governed by the Efremov-Radyushkin-Brodsky-Lepage (ERBL) evolution kernel where the one- and two-loop results are available in [25, 26] and [27–31], respectively. The three-loop ERBL kernel has been computed recently in both the naive dimensional regularization (NDR) [32] and the Larin scheme [33] from conformal symmetry.

The CF  $T_2$  can be expanded perturbatively in the form

$$T_2 = \sum_{\ell=0}^{\infty} a_s^\ell T_2^{(\ell)}, \quad a_s \equiv \frac{\alpha_s}{4\pi} = \frac{g_s^2}{(4\pi)^2} \quad (5)$$

with  $g_s$  being the strong coupling constant. The explicit expressions for the tree-level  $T_2^{(0)}$ , one-loop  $T_2^{(1)}$ , and two-loop  $T_2^{(2)}$  coefficient functions in the  $\overline{\text{MS}}(\text{NDR})$ -scheme can be found in the addendum of [22].

As a physical observable, the pion TFF  $F_{\gamma\pi}(Q^2)$  is evidently independent of the factorization scale  $\mu_F$ , hence yielding an importance constraint for the TFF computed with CF up to  $\ell$ -loops.

$$\frac{d}{d \ln \mu} F_{\gamma\pi}^{(\ell)}(Q^2, \mu) = \mathcal{O}(\alpha_s^{\ell+1}). \quad (6)$$

It is mandatory to evaluate the resummation improved  $F_{\gamma\pi}(Q^2)$  with the RG-evolution kernel of the pion LCDA expanded up to the order of one-loop higher than the CF. We will follow this procedure in the next section by employing the full two-loop CF and the three-loop evolution kernel [32] to obtain the complete next-to-next-to-leading-logarithm prediction (NNLL) for the TFF.

### 3 Numerical analysis

To analyze the accessibility of  $\phi_\pi(x, \mu_F)$  via the experimental data, we will employ three phenomenologically acceptable models. These models are motivated by accommodating the available information on the LCDA from the various QCD methods. It is helpful to decompose  $\phi_\pi(x, \mu_F)$  in terms of the Gegenbauer polynomials  $C_{2n}^{3/2}(2x-1)$  which diagonalize the one-loop ERBL kernel, namely,

$$\phi_\pi(x, \mu_F) = 6x\bar{x} \left[ 1 + \sum_{n=1}^{\infty} a_{2n}(\mu_F) C_{2n}^{3/2}(2x-1) \right], \quad (7)$$

<sup>1</sup>We assume the leading-power approximation hereafter unless stated otherwise.

where  $\bar{x} = 1 - x$ ,  $a_{2n}(\mu_F)$  are known as the Gegenbauer moments of the pion LCDA. Note that only the polynomial  $C_{2n}^{3/2}(2x - 1)$  with an even index contributes due to  $\phi_\pi(x, \mu_F) = \phi_\pi(\bar{x}, \mu_F)$  as a consequence of the charge symmetry. The renormalization group analysis demonstrates that  $a_{2n}(\mu_F) \rightarrow 0$  as  $\mu_F \rightarrow \infty$  hence giving rise to the asymptotic pion LCDA

$$\phi_\pi^{\text{asy}}(x) \equiv 6x\bar{x}. \quad (8)$$

It is instructive to take  $\phi_\pi^{\text{asy}}(x, \mu_0)$  as a legitimate, albeit a crude model for the leading-twist pion LCDA at a reference scale  $\mu_0$ . Employing the factorization formula Eq. (3) at the two-loop level and setting  $\mu = \mu_0$ , we find

$$F_{\gamma\pi}^{\text{asy}}(Q^2, \mu_0) = \frac{(e_u^2 - e_d^2)f_\pi}{\sqrt{2}Q^2} \left\{ 6 - 30a_s C_F - a_s^2 C_F \left[ \beta_0 ((31 + 12L_0)\zeta_2 + 6\zeta_3 + 7) \right. \right. \\ \left. \left. + C_F \left( 24(\zeta_2 + \zeta_3)L_0 + 42\zeta_4 + 54\zeta_3 + 37\zeta_2 - \frac{85}{2} \right) - \frac{1}{N_c} (6\zeta_4 - 12\zeta_3 - 2\zeta_2 + 13) \right] \right\}, \quad (9)$$

where  $L_0 \equiv \ln(\mu_0^2/Q^2)$ . Note that the appearance of  $L_0$  does not indicate the scale dependence of the TFF as the ERBL kernel has to be applied to  $\phi_\pi(x, \mu_0)$  to facilitate the scale variation.

It is conventional to construct the phenomenological models at a common reference scale of  $\mu_0 = 2$  GeV. The LCDA is then evolved to the appropriate factorization scale  $\mu_F$  to make predictions for the TFF via Eq. (3). We are now ready to explore the numerical consequences of three more elaborated models of the pion LCDA as listed below in greater detail.

$$\text{Model I :} \quad \phi_\pi(x, \mu_0) = \frac{\Gamma(2 + 2\alpha_\pi)}{\Gamma^2(1 + \alpha_\pi)} (x\bar{x})^{\alpha_\pi}, \quad (10)$$

$$\text{with } \alpha_\pi(\mu_0) = 0.422_{-0.067}^{+0.076};$$

$$\text{Model II :} \quad \{a_2, a_4\}(\mu_0) = \{0.269(47), 0.185(62)\}, \\ \{a_6, a_8\}(\mu_0) = \{0.141(96), 0.049(116)\};$$

$$\text{Model III :} \quad \{a_2, a_4\}(\mu_0) = \{0.203_{-0.057}^{+0.069}, -0.143_{-0.087}^{+0.094}\}.$$

The general ansatz of Model I is inspired by the AdS/QCD correspondence [34] with the specific value of  $\alpha_\pi(\mu_0)$  determined from the most recent lattice result  $a_2(2 \text{ GeV}) = 0.116_{-0.020}^{+0.019}$  [1]. Model II with truncated expansion in Gegenbauer polynomials is constructed by matching the pion electromagnetic form factor in the space-like region to the modified dispersion integral, modulus of the time-like contribution [35]. The intervals of  $a_2$  and  $a_4$  in Model III [36–38] are determined also from the QCD sum rules with the non-local quark condensate responsible for the finite correlation length of vacuum fluctuations [39]. To implement the three-loop evolution of  $\phi_\pi(x, \mu)$  [32], we will take into account the Gegenbauer moments up to  $a_{14}(\mu)$  for the “holographic”-type Model I, which is sufficient for our numerical analysis as demonstrated in [40].

Clearly, all three models for  $\phi_\pi(x, \mu_0)$  are somewhat unsatisfactory, as none of them are subject to sufficient experimental constraints. This can be partially understood from the fact that all previous data on the pion TFF are either limited to the small  $Q^2$  region invalidating the leading-power approximation (e.g., the CLEO collaboration [8], or possessing large errors with contradictory measurements (e.g., BaBar [7] vs Belle [9] as illustrated in Fig. 1). It is therefore without doubt that an independent measurement of the TFF is vital for settling the considerable discrepancy between the BaBar and Belle data as displayed in Fig. 1.

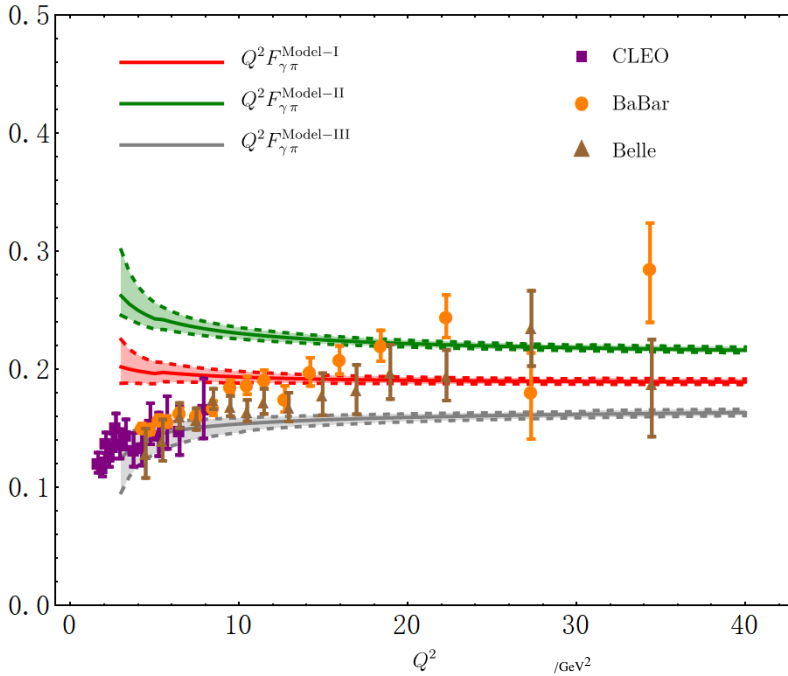


**Figure 1.** Theory predictions of the TFF  $\gamma\gamma^* \rightarrow \pi^0$  for the three models presented in (10), including the NNLL QCD prediction of the leading, as well as the sub-leading power corrections from the higher-twist pion and photon DAs [41]. The color bands are due to variation of the scale  $\mu$  in Eq. (4). For a comparison, we also display the experimental measurements from the CLEO [8] (purple squares), BaBar [7] (orange circles) and Belle [9] (brown spades) Collaborations.

Based on the three acceptable models presented in Eq. (10), we are now prepared to demonstrate the theory predictions for the pion TFF, which are further confronted with the available experimental data currently, as shown in Fig. 1. Here we have also taken into account the sub-leading power corrections generated by higher-twist pion LCDA and the collinear photon distribution amplitudes [41]. Such corrections are systematically negligible for  $Q^2 \gtrsim 20 \text{ GeV}^2$  [22] consistent with the established hierarchy pattern of the pion TFF. The color bands, which are obtained from the “default” range of the scale variable  $\mu^2 = \langle x \rangle Q^2$  with  $1/4 \leq \langle x \rangle \leq 3/4$  [40], reveals the perturbative uncertainty of the NNLL resummation improved leading-power contribution (i.e., Eq. (3)). Note that in Fig. 1, the quoted numerical uncertainties of each model in Eq. (10) are not taken into account to highlight the potentiality of the experimental data in resolving the model uncertainties of  $\phi_\pi(x, \mu_0)$ .

The snapshot of a well-separated TFF prediction is particularly encouraging as it demonstrates the power of the precision measurement of the pion TFF in disentangling various models of  $\phi_\pi(x, \mu_0)$ . As these models are established by speculating quantitatively the intricate dynamics of the leading-twist DA from different perspectives, a better constrained  $\phi_\pi(x, \mu_0)$  is indispensable for unveiling the partonic structures of the neutral pion system. We emphasize again that in order to properly extract the leading-twist pion LCDA  $\phi_\pi(x, \mu_0)$ , it is crucial to have access to the large kinematic regime of  $Q^2 \gtrsim 20 \text{ GeV}^2$  where the sub-leading power contributions are sufficiently suppressed. This criteria is met by the proposed design

of CEPC with high luminosity, efficient neutral particle reconstruction technique, and high momentum resolution [2].

We point out that based on the blueprint of the CEPC, it is also advisable to measure the radiative-leptonic decay channel of the neutral pion  $\pi^0 \rightarrow e^+e^-\gamma$  with tagging, in which case all discussions in this work fully apply. In addition, precision measurements for the double-virtual  $\gamma^*\gamma^* \rightarrow \pi^0$  form factor are also highly appreciated, since it serves as a fundamental ingredient to determine the hadronic light-by-light (HLbL) scattering contribution entering the prediction of the muon anomalous magnetic moment in the dispersion framework.

## 4 Conclusions

In summary, we have endeavored to illustrate the accessibility of the leading-twist pion LCDA via the pion TFF in the large- $Q^2$  region at the envisioned CEPC. Our analysis draws a positive conclusion. The significance of an updated experimental input was addressed by employing three representative models of the twist-two pion LCDA at the NNLL accuracy. A clean separation of the TFF predictions from various models is observed. This is particularly promising as it permits the extraction of the  $\phi_\pi(x, \mu)$  with much less ambiguity, which is important for shedding lights on the partonic dynamics of the composite hadronic state.

## Acknowledgements

We would like to thank Nico G. Stefanis and all the conveners of Section B (Light Quarks) for the kind invitation as well as the organizing committee for organizing such a wonderful conference. We are further grateful to Jing Gao and Tobias Tuber for a very fruitful collaboration on [22]. Y.J. acknowledges the support of Collaborative Research Center TRR110/2 funded by the Deutsche Forschungsgemeinschaft (DFG, German Research Foundation) under grants 196253076. Y.M.W. is grateful for the support from the National Natural Science Foundation of China with Grant No. 11675082, 11735010 and 12075125, and the Natural Science Foundation of Tianjin with Grant No. 19JCJQJC61100.

## References

- [1] G.S. Bali, V.M. Braun, S. Bürger, M. Göckeler, M. Gruber, F. Hutzler, P. Korcyl, A. Schäfer, A. Sternbeck, P. Wein (RQCD), *JHEP* **08**, 065 (2019), [Addendum: *JHEP* **11**, 037 (2020)], [1903.08038](#)
- [2] M. Ruan et al., *Eur. Phys. J. C* **78**, 426 (2018), [1806.04879](#)
- [3] Y. Ji, A. Vladimirov, *Eur. Phys. J. C* **79**, 319 (2019), [1901.06960](#)
- [4] J.M. Cornwall, *Phys. Rev. Lett.* **16**, 1174 (1966)
- [5] D.J. Gross, S.B. Treiman, *Phys. Rev. D* **4**, 2105 (1971)
- [6] S.J. Brodsky, T. Kinoshita, H. Terazawa, *Phys. Rev. D* **4**, 1532 (1971)
- [7] B. Aubert et al. (BaBar), *Phys. Rev. D* **80**, 052002 (2009), [0905.4778](#)
- [8] J. Gronberg et al. (CLEO), *Phys. Rev. D* **57**, 33 (1998), [hep-ex/9707031](#)
- [9] S. Uehara et al. (Belle), *Phys. Rev. D* **86**, 092007 (2012), [1205.3249](#)
- [10] V.M. Braun, A.N. Manashov, S. Moch, J. Schoenleber, *JHEP* **09**, 117 (2020), [2007.06348](#)
- [11] V.M. Braun, Y. Ji, A.N. Manashov, *JHEP* **03**, 051 (2021), [2011.04533](#)
- [12] V.M. Braun, Y. Ji, J. Schoenleber, *Phys. Rev. Lett.* **129**, 172001 (2022), [2207.06818](#)
- [13] H.n. Li, Y.L. Shen, Y.M. Wang, *Phys. Rev. D* **85**, 074004 (2012), [1201.5066](#)

- [14] H.n. Li, Y.M. Wang, JHEP **06**, 013 (2015), 1410.7274
- [15] C.D. Lü, Y.L. Shen, C. Wang, Y.M. Wang (2022), 2202.08073
- [16] F. del Aguila, M.K. Chase, Nucl. Phys. B **193**, 517 (1981)
- [17] E. Braaten, Phys. Rev. D **28**, 524 (1983)
- [18] E.P. Kadantseva, S.V. Mikhailov, A.V. Radyushkin, Yad. Fiz. **44**, 507 (1986)
- [19] H.n. Li, G.F. Sterman, Nucl. Phys. **B381**, 129 (1992)
- [20] I.V. Musatov, A.V. Radyushkin, Phys. Rev. **D56**, 2713 (1997), hep-ph/9702443
- [21] H.N. Li, Y.L. Shen, Y.M. Wang, JHEP **01**, 004 (2014), 1310.3672
- [22] J. Gao, T. Huber, Y. Ji, Y.M. Wang, Phys. Rev. Lett. **128**, 062003 (2022), 2106.01390
- [23] V.M. Braun, A.N. Manashov, S. Moch, J. Schoenleber (2021), 2106.01437
- [24] P.A. Zyla et al. (Particle Data Group), PTEP **2020**, 083C01 (2020)
- [25] A.V. Efremov, A.V. Radyushkin, Phys. Lett. B **94**, 245 (1980)
- [26] G.P. Lepage, S.J. Brodsky, Phys. Rev. D **22**, 2157 (1980)
- [27] M.H. Sarmadi, Phys. Lett. B **143**, 471 (1984)
- [28] F.M. Dittes, A.V. Radyushkin, Phys. Lett. B **134**, 359 (1984)
- [29] G.R. Katz, Phys. Rev. D **31**, 652 (1985)
- [30] S.V. Mikhailov, A.V. Radyushkin, Nucl. Phys. B **254**, 89 (1985)
- [31] A.V. Belitsky, D. Mueller, A. Freund, Phys. Lett. B **461**, 270 (1999), hep-ph/9904477
- [32] V.M. Braun, A.N. Manashov, S. Moch, M. Strohmaier, JHEP **06**, 037 (2017), 1703.09532
- [33] V.M. Braun, A.N. Manashov, S. Moch, M. Strohmaier, Phys. Rev. D **103**, 094018 (2021), 2101.01471
- [34] S.J. Brodsky, G.F. de Teramond, Phys. Rev. D **77**, 056007 (2008), 0707.3859
- [35] S. Cheng, A. Khodjamirian, A.V. Rusov, Phys. Rev. D **102**, 074022 (2020), 2007.05550
- [36] A.P. Bakulev, S.V. Mikhailov, N.G. Stefanis, Phys. Lett. B **508**, 279 (2001), [Erratum: Phys.Lett.B 590, 309–310 (2004)], hep-ph/0103119
- [37] S.V. Mikhailov, A.V. Pimikov, N.G. Stefanis, Phys. Rev. D **93**, 114018 (2016), 1604.06391
- [38] N.G. Stefanis, Phys. Rev. D **102**, 034022 (2020), 2006.10576
- [39] S.V. Mikhailov, A.V. Radyushkin, Phys. Rev. D **45**, 1754 (1992)
- [40] S.S. Agaev, V.M. Braun, N. Offen, F.A. Porkert, Phys. Rev. D **83**, 054020 (2011), 1012.4671
- [41] Y.M. Wang, Y.L. Shen, JHEP **12**, 037 (2017), 1706.05680